RESEARCH PAPER

RNA Biology 12:5, 514–524; May 2015; © 2015 Taylor & Francis Group, LLC

The thumb subdomain of yeast mitochondrial RNA polymerase is involved in processivity, transcript fidelity and mitochondrial transcription factor binding

Gilberto Velazquez[1], Rui Sousa[2], and Luis G Brieba[1,*]

[1]Laboratorio Nacional de Genómica para la Biodiversidad; Centro de Investigación y de Estudios; Irapuato, Guanajuato, México; [2]Department of Biochemistry; University of Texas Health Science Center; San Antonio, TX USA

Keywords: fidelity, mitochondrial RNA polymerase, processivity

Abbreviations: ymtRNP, yeast mitochondrial RNA polymerase; Mtf1, Mitochondrial Transcription Factor

Single subunit RNA polymerases have evolved 2 mechanisms to synthesize long transcripts without falling off a DNA template: binding of nascent RNA and interactions with an RNA:DNA hybrid. Mitochondrial RNA polymerases share a common ancestor with T-odd bacteriophage single subunit RNA polymerases. Herein we characterized the role of the thumb subdomain of the yeast mtRNA polymerase gene (RPO41) in complex stability, processivity, and fidelity. We found that deletion and point mutants of the thumb subdomain of yeast mtRNA polymerase increase the synthesis of abortive transcripts and the probability that the polymerase will disengage from the template during the formation of the late initial transcription and elongation complexes. Mutations in the thumb subdomain increase the amount of slippage products from a homopolymeric template and, unexpectedly, thumb subdomain deletions decrease the binding affinity for mitochondrial transcription factor (Mtf1). The latter suggests that the thumb subdomain is part of an extended binding surface area involved in binding Mtf1.

Introduction

Mitochondrial RNA polymerases are evolutionary related to the T-odd bacteriophage single subunit RNA polymerases.[1,2] Crystal structures of the human mitochondrial RNA polymerase (hmtRNAP) and T7 RNA polymerase (T7RNAP) reveal the structural conservation of the C-terminal or polymerase domain which resembles a cupped right hand in which specific subdomains dubbed palm, fingers and thumb are arranged to interact with an RNA:DNA hybrid, bind NTPs and catalyze rNMP incorporation.[3-6] In comparison to T7RNAP, yeast mitochondrial RNA polymerase (ymtRNAP) and hmtRNAP have an extra N-terminal domain implicated in transcription-translation coupling.[7,8] This N-terminal domain, folds as a pentatricopeptide repeat that interacts with the nascent RNA and possibly with translation associated proteins.[4] Structural elements like the promoter recognition and DNA intercalating β-hairpin loops fulfill analogous functions in promoter recognition and opening in ymtRNAP and T7RNAP.[9-11] In contrast to phage RNAPs, mitochondrial RNAPs require accessory factors for promoter recognition, melting and termination.[12,13]

T7 DNA and RNA polymerases achieve complex stability while allowing lateral movement via their thumb subdomains. In T7DNAP, an extended loop of the thumb subdomain interacts with thioredoxin to present a large surface that interacts with DNA, and in T7RNAP the thumb subdomain is a flexible element important for processivity, stability of the late initiation and elongation complexes, and recognition of Class II termination sequences.[14-16] Mutagenesis studies of the thumb subdomain in hmtRNAP shown that this structural element contributes to the stability of the elongation complex.[3] The thumb subdomain of nucleic acid polymerases has functions in addition to complex stability, such as maintain frame-shift fidelity on homopolymeric runs,[17] primer delivery in T7 DNAP,[18] and recognition of Class II termination sequences in T7 RNAP.[19] In comparison to human mitochondrial and T7 RNAPs, little is known about roles of the thumb subdomain during transcription.[3,14,19] In order to fill this gap, we present an extensive characterization of the thumb subdomain of ymtRNAP and its role in transcription complex stability, processivity and frame-shift fidelity.

*Correspondence to: Luis G Brieba; Email: lgbrieba@langebio.cinvestav.mx
Submitted: 11/28/2014; Revised: 01/21/2015; Accepted: 01/23/2015
http://dx.doi.org/10.1080/15476286.2015.1014283

Results

The thumb subdomains of ymtRNAP and T7 RNAP share low amino acid sequence identity

A structure-based sequence alignment of the thumb subdomain of T7RNAP, hmtRNAP and ymtRNAP shows that the 2 α helices that comprise their thumb subdomains (L and N according to the crystal structure of the T7RNAP elongation complex) only share 15% in amino acid identity (**Fig. 1A**). Since the poor sequence conservation meant that we could not identify residues in ymtRNAP that would correspond to functionally assigned residues in the T7RNAP thumb, and because the thumb subdomain consists of more than 45 residues, we created 3 constructs in which we replaced 2 positively charged residues with alanine in different regions of the thumb subdomain. Construct TH_A mutates residues R780 and K783, located at the N-terminal tip of thumb subdomain; construct TH_B mutates amino acids K787 and K792 at the middle of the predicted α helix N; and construct TH_C mutates residues R797 and R800 located at the C-terminal end of α helix N of the thumb subdomain. As the thumb subdomain is a flexible subdomain that encircles the RNA-DNA hybrid in elongation complexes of T7RNAP and hmtRNAP,[3,20] we constructed 2 deletion mutants of 5 and 11 amino acids in the putative loop that connects αL and αN (TH_Δ5 and TH_Δ11). Misfolded ymtRNAPs have a strong tendency to aggregate. Our point and deletion mutants present a similar elution profile in a S200 gel filtration column, indicating that they are properly folded and that the deletion mutants only cause local changes in structure (data not shown).

Alanine Scanning and deletion mutants increase abortive termination

To determine the effect of mutations in the thumb subdomain we analyzed the transcription pattern for the wild-type and mutants in a 35-mer run-off transcription reaction using the double-stranded mitochondrial 14S rRNA promoter in the presence of 20-fold molar excess of Mtf1. Abortive and run-off products were resolved on 20% polyacrylamide denaturing gels. All thumb mutants were active and efficiently synthesized run-off transcripts (**Fig. 2A**), indicating that mutations in the thumb subdomain did not alter the active site of the enzyme. Point and deletion mutants synthesized longer RNA products when compared to

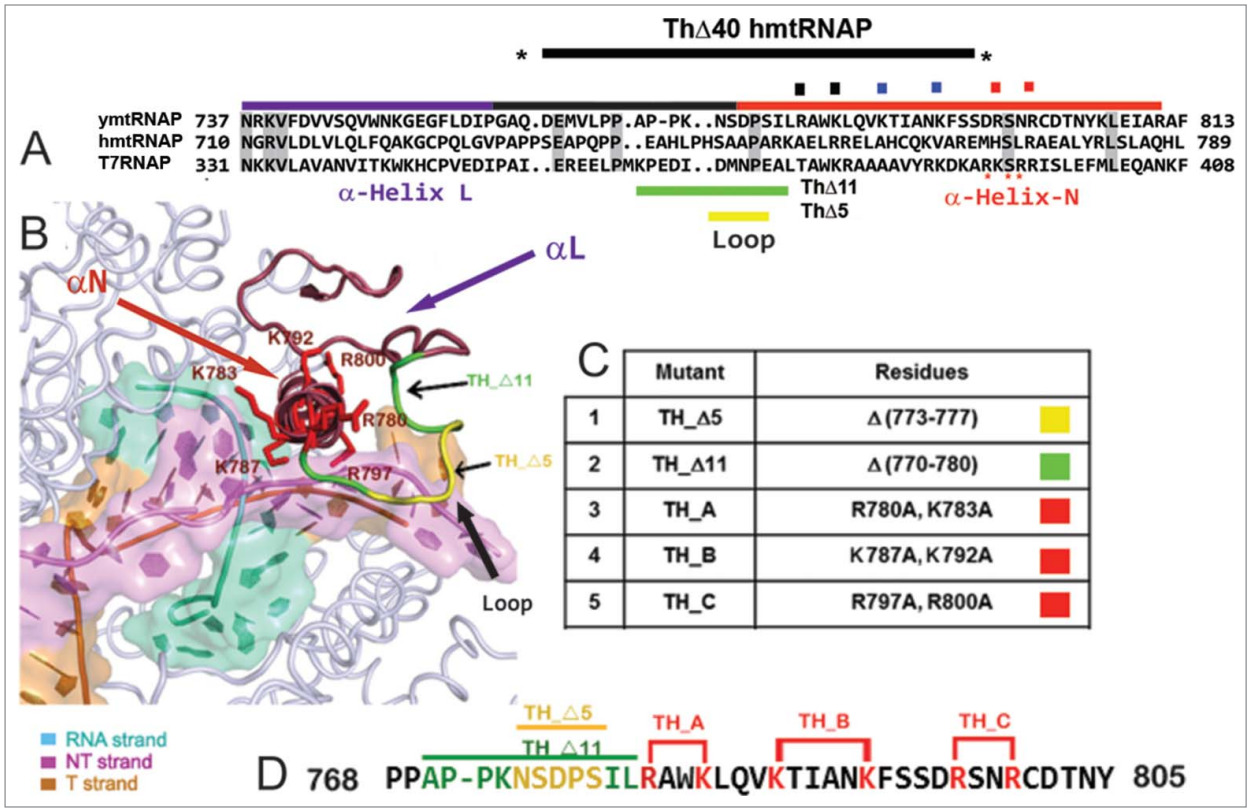

Figure 1. Structure-based sequence alignment of single subunit RNAPs and location of thumb subdomain mutants. (**A**) Structure based sequence alignment of single subunit RNAPs thumbs, showing the amino acid sequence of the thumb subdomains of T7RNAP, and yeast (ymtRNAP) and human (hmtRNAP) mitochondrial RNAP. Conserved residues are highlighted in gray and the 3 positively charged amino acids in the center of αN, are indicated by a red asterisk. The amino acids that comprise α-helices L and N are highlighted by purple and red lines respectively. The red line indicates the amino acids corresponding to a 40 amino acid deletion of hmtRNAP[3] (**B**) Structural model of an elongation complex of ymtRNAP showing the thumb subdomain. α-helices L and N are in purple. Alanine substituted residues are shown in stick representation, deleted regions are colored in yellow (TH_Δ5) and green (TH_Δ11). RNA is in cyan, Non template (NT) strand in magenta and Template (T) strand in orange. (**C**). Table indicating the location of residues for the alanine substitution and deletion mutants generated in this work. (**D**). Expanded view of the thumb subdomain mutants.

the wild-type enzyme. These products may represent addition of non-templated NTPs or misincorporation (**Fig. 2A, lanes 2 to 6**). As previously observed, wild-type ymtRNAP synthesized abortive products, from 2 to 8-mers, before beginning processive transcription (**Fig. 2A, lane 1**). As the synthesis of the more abundant 2-mer and run-off transcripts may mask other products, the quantification of the abortive synthesis focuses on products from 3 to 11 nts (**Fig. 2B**). Point mutants, with the exception of TH_A, presented a decrease in the amount of abortive 2-mers (**Fig. 2A, lanes 1 to 4**). In contrast to the synthesis of 2-mers, the TH_B mutant increased the synthesis of abortive 3-mers by 5-fold, TH_A increased synthesis of 4-mer by 2-fold, whereas TH_C and the deletion mutants did not increase the synthesis of abortive transcripts. Mutants TH_Δ5 and TH_Δ11 synthesized fewer abortive transcripts, and TH_Δ11 synthesized aberrant short transcripts that may be the result of misincorporation due to template strand slippage (**Fig. 2A, lanes 5 and 6**).

All mutants presented an increase in abortion and termination products after the synthesis of a 6-mer. There were multiple differences in the transcription patterns between the thumb mutants during elongation. TH_A and TH_B present a transcription termination pattern centered at ~22 nts whereas TH_C termination is centered at ~11-nts, and the deletion mutants increase termination between 24 to 33 nts before reaching the end of the template. These results indicate that mutations at the thumb subdomain decrease the overall stability of the initial transcription (ITC) and elongation complexes (EC).

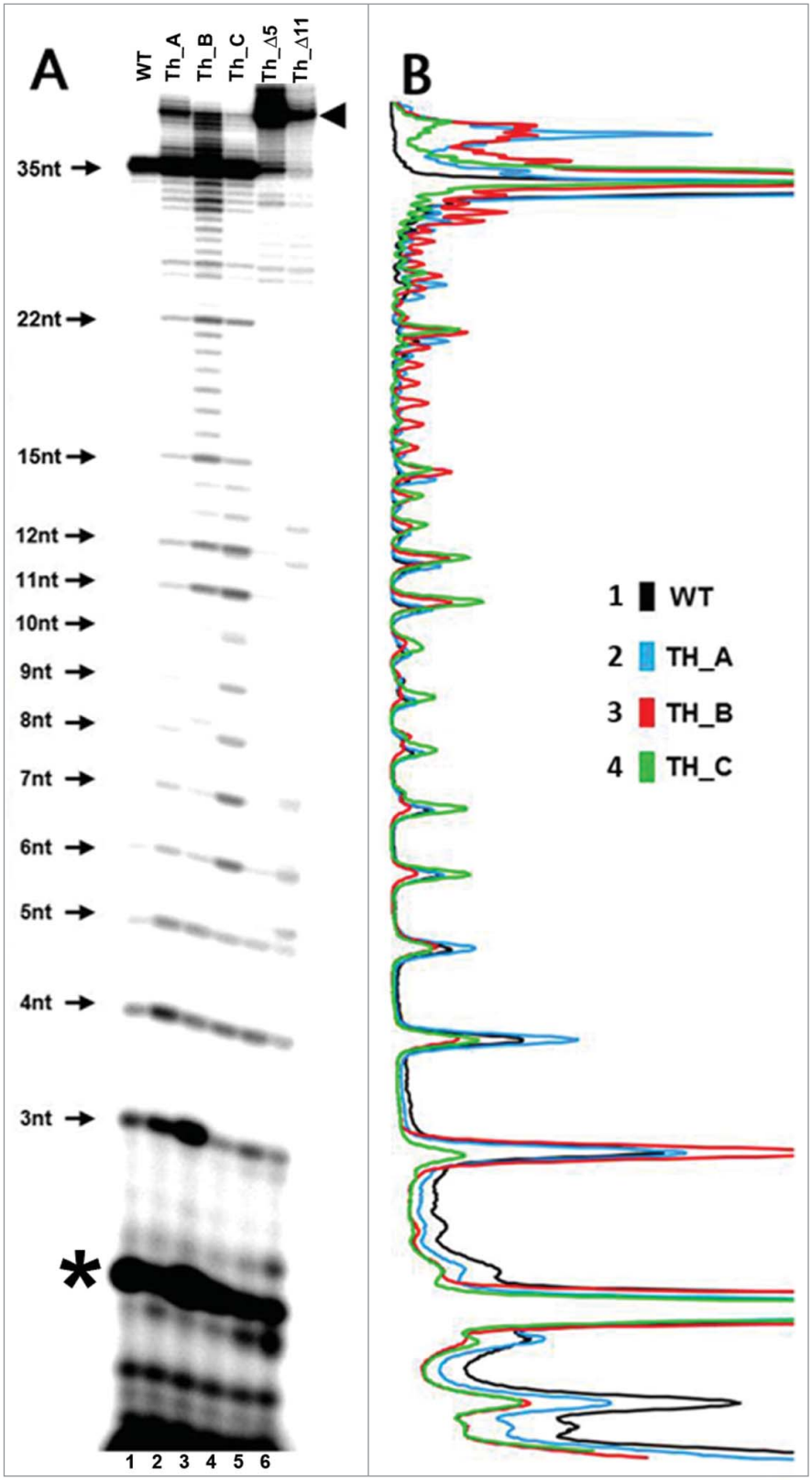

Figure 2. Thumb mutants increase abortive and early termination transcripts. (**A**) Denaturing 15% acrylamide, 7M urea gel showing a run-off transcription assay of wild-type and mutant ymtRNAPs. RNAPs were present at a concentration of 0.1 μM with 2 μM Mtf1. The 55 nt long 14S rRNA promoter was at 0.01 μM. The length of the run-off (35-mer) and abortive transcripts (2–9 mers) as well as early termination products (10–22 mers) are indicated. Lane 1. Wild-type enzyme; Lane 2, TH_A mutant; Lane 3, TH_B mutant; Lane 4, TH_C mutant; Lane 5, TH_ Δ5 and lane 6 TH_Δ11 mutant. The RNA products are indicated with arrows. Aberrant transcription products are indicated by a triangle. (**B**) Quantification of abortive and early termination products for the mutants TH_A (cyan), TH_B (red), TH_C (green) compared with the wild-type enzyme (black). The intensity of the bands was normalized with respect to the run-off product of each enzyme (at 35-mer).

Alanine Scanning and deletion mutants decrease the stability of early and late transcription initiation complexes

To further evaluate the effect of mutations in the thumb subdomain on the stability of transcription complexes, we measured the steady-state transcript synthesis of complexes halted at the 2-, 7-, and 12-mer points by NTP omission. Under such conditions the rate of transcript synthesis is limited by the stability (turnover) transcription complexes if the rate of complex dissociation is slower than the sum of the rates of the other steps in the reaction.[14,21] The TH_A, deletion mutants and WT polymerases exhibited similar amounts of 2-mer synthesis (**Fig. 3A, B**), while the TH_B and TH_C mutants exhibited a modest 2.5-fold increase in 2-mer synthesis relative to WT (**Fig. 3A, B**). These data indicate either that the thumb subdomain is not important for the stability of the 2-mer complex or that, as in T7RNAP, the 2-mer complex is so unstable that 2-mer synthesis is not limited by complex turnover[14]. In contrast, there was a large increase in transcript synthesis for all mutants halted at the 7-mer stage, especially for TH_B and TH_Δ11 which increased synthesis rates by 7 and 9-fold, respectively. This indicates that the thumb subdomain is involved in stabilizing the late ITC (RNA > 5 mer), and is consistent with the idea that short (2–3 mer) transcripts readily dissociate from the transcription complex, but that upon growth of the RNA chain and formation of an extended RNA:DNA hybrid, the complex is stabilized by the thumb subdomain as in other single-subunit RNA polymerases.[3,14]

Mutations in the thumb subdomain destabilize elongation complexes in supercoiled, but not linearized, templates

To determine if thumb deletions destabilize the elongation complex ($_{EC}$), we measured the turnover rate of 12-mer elongation complexes on supercoiled and linear templates (pUC19–14S). We found that the turnover rate of the thumb mutants was similar to the wild-type polymerase on a linear template (**Fig. 4A, B**). However, when we measured the turnover rate on a supercoiled template, only the complex formed with the wild-type enzyme was as stable as on a linear template complex. TH_A and TH_B strongly destabilized these complexes, while TH_C and TH_Δ5 had lesser effects on stability (**Fig. 4C, D**). This surprising result is entirely consistent with previous

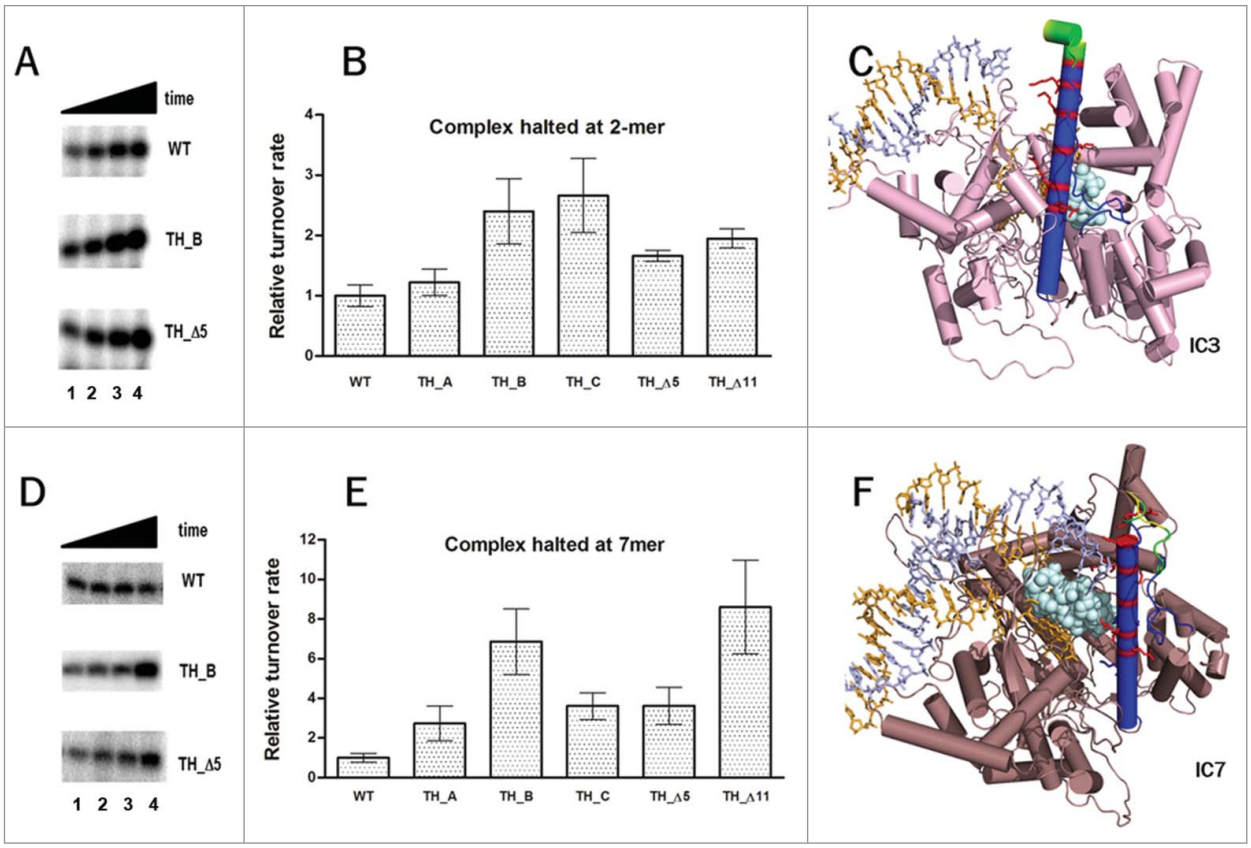

Figure 3. Effect of the thumb subdomain on the stability of the 2-mer and 7-mer complexes measured by steady-state transcript synthesis. (**A and D**) Representative turnover experiments of transcription reactions with wild-type and mutant ymtRNAPs in which transcript extension was limited to 2 nts (A) or 7nts (D) by inclusion of only ATP, or ATP and UTP, respectively. Time points were at 2, 8, 16 and 32 minutes. Mitochondrial RNAPs were at 10 nM and Mtf1 at 200 nM, with synthetic 14s promoter at 20 nM. (**B and E**) Relative turnover rates for 2-mer and 7-mer synthesis. The relative turnover rate was calculated from the slope of the accumulation of transcription products in (**A**). Error bars indicate the ranges from 3 independent experiments. (**C and F**) Structural model of ymtRNAP in the early initiation complex (ITC3) or late initiation complex (ITC7) based on T7RNAP ITC structures. The thumb subdomain is in blue, point mutations in red, deletion mutants in yellow (5 amino acids) or green (11 amino acids). Non-template DNA strand is in light purple, the template strand is in orange, and RNA is represented as blue spheres.

observations with T7RNAP that similarly showed that thumb mutations in T7RNAP destabilizes ECs on supercoiled, but not linear, templates[21]. This was shown to be due to formation of extended RNA:DNA hybrids on supercoiled templates which resulted in disruption of T7RNAP interactions with the nascent single-stranded RNA. The combination of loss of nascent RNA:RNAP contacts with thumb mutations led to exceptional $_{EC}$ instability. Our results indicate that the ymtRNAP thumb is similarly involved in $_{EC}$ stability.

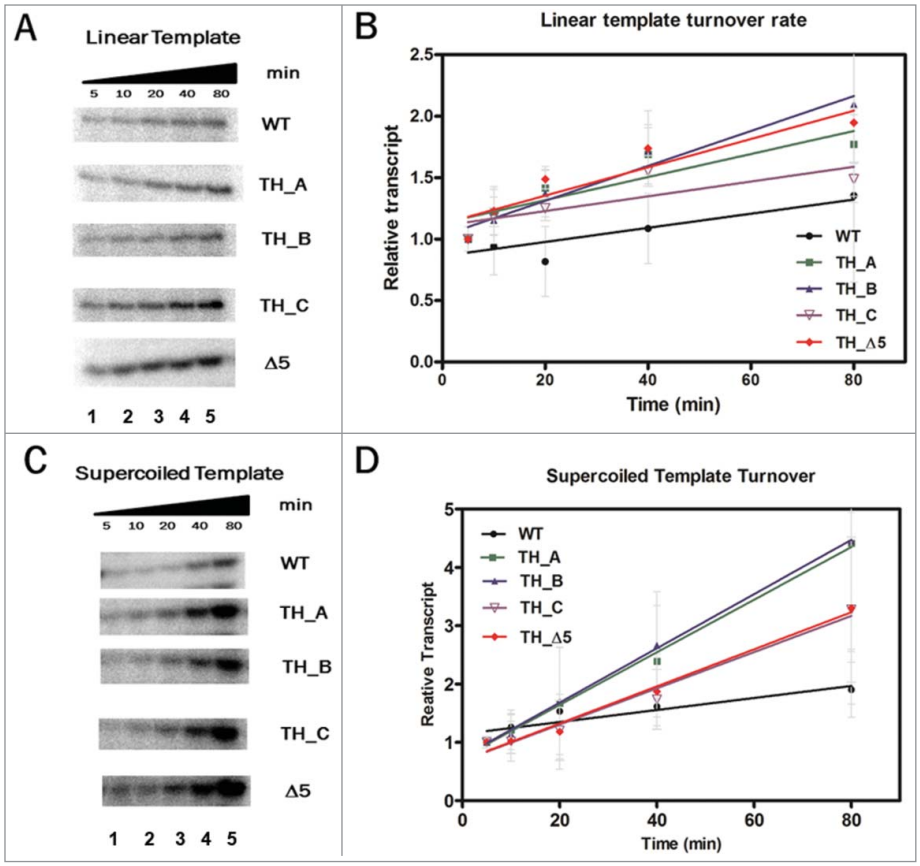

Figure 4. Effect of the thumb subdomain on the stability of the 12-mer elongation complex as measured by steady-state transcript synthesis. (**A and C**). Representative experiment for measuring the turnover of wild-type and mutant RNAPs during synthesis of 12-mer transcripts on Hin*d* III linearized or supercoiled pUC-14S templates with 0.5 mm ATP, GTP, and 3′-dCTP. Proteins and template concentrations are as in **Figure 3**. (**B and D**). Steady-state rates of 12-mer synthesis on linear (**A and B**) or supercoiled (**C and D**) templates. Error bars indicate SE for 3 independent experiments.

Mutations of the thumb subdomain decrease synthesis of long transcripts

Once ymtRNAP synthesizes a transcript longer than ~9 nts it switches from abortive to processive RNA synthesis. During processive synthesis the RNA polymerase elongates the RNA chain without falling off the template.[8] Since point and deletion thumb mutant results unstable late ITC and ECs we were interested in determining if the mutants show a decrease in the synthesis of long transcripts. We measured the total amount of RNA product from a linearized template that generates a transcript of 2.7 kb. The amount of full-length transcript synthesized by the thumb mutants ranged from 19 to 25% of that transcribed by wild-type ymtRNAP (**Fig. 5, lanes 1 to 6**). In contrast, on a template that allows synthesis of a 34-mer transcript, the wild-type and thumb mutants synthesize similar amounts of run-off products. This specific deficit of the thumb mutants in synthesizing long runoff transcripts indicate that these mutants reduce ymtRNAP processivity, most likely by increasing the rate at which the $_{EC}$ dissociates so that fewer complexes reach the end of a long template.

Deletion mutants affect frameshift fidelity

Mutations in the thumb subdomain of DNA polymerases decrease frameshift fidelity but not base substitution fidelity.[17] Because thumb ymtRNAP mutants synthesize longer transcripts in a 35-mer run-off assay (**Fig. 2A**), we decided to test if mutations in the thumb subdomain have any effect on fidelity of transcription of homopolymeric templates that promote template:RNA slippage. The experiment consisted of incubating preassembled DNA:RNA scaffolds in which the templating bases consisted of runs of increasing numbers of thymines, from 1 (1T) to 6 (6T). Fidelity is assayed in individual transcription reactions in the presence of ATP, CTP, GTP or UTP. In transcription reactions using a scaffold with one thymine in the presence of ATP only, wild-type and deletion mutants incorporate 1 or 3 AMP (T7RNAP incorporated 2–3 AMPs on this template; **Fig. 6A, lane 22**). However, no misincorporation of GTP, UTP or CTP was observed when these NTPS were added (**Fig. 6A, lanes 2,7,12,17**), indicating that misincorporation remains low in the reactions with thumb mutants. On a template with 2 thymines, the wild-type, thumb mutants and T7 RNAPs incorporated 4 AMPs (**Fig. 6B, lanes 2,7,12,17**). However, in contrast to the ymtRNAPs, T7 RNA polymerase also misincorporated GTP and CTP (**Fig. 6B, lanes 21–24**). On a template with 3 thymines, all mutants, except TH_Δ11, incorporated 4–6 AMPs. The TH_Δ11 mutant synthesized a ladder of 4–11 AMPs (**Fig. 6C, lanes 16**) and also misincorporated GMP (**Fig. 6C, lanes 2,7,12,17**). With a run of 5 thymines, wild-type and mutant RNAPs incorporated 6–7 AMPs, while the TH_Δ11 mutant synthesized a ladder of 7–18 AMPs, and also misincoporated GMP. On a run of 6 thymines, the wild-type enzyme incorporated 7–8 AMPs, the TH_B mutant incorporated 7–9 AMPs, TH_Δ5 incorporated primarily 8 AMPs but also produced a ladder of 8 to 12 AMPs, while TH_Δ11 produced a ladder of 8 to >20 AMPs.

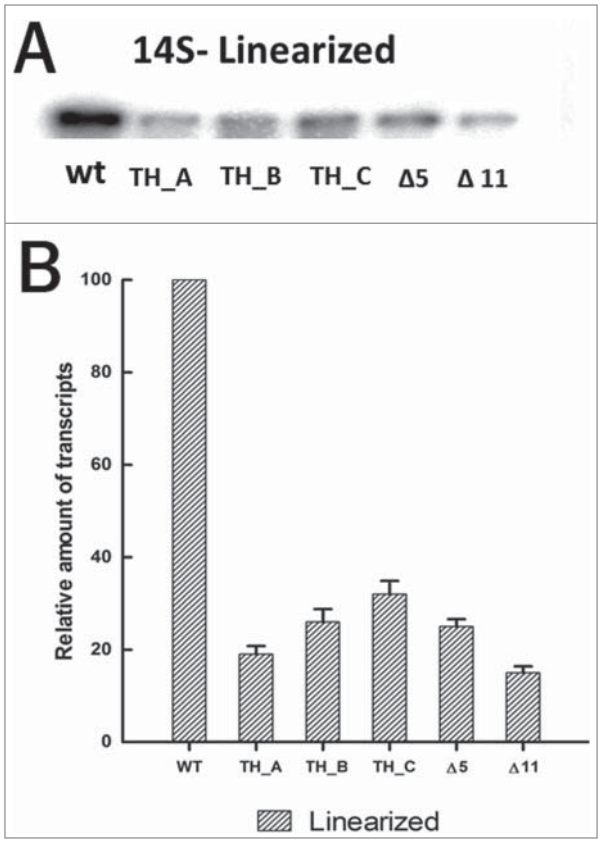

Figure 5. ymtRNAP thumb mutants decrease synthesis of long transcripts. (**A**) Representative experiment for wild-type and modified RNAPs measuring the ability to synthesize transcripts of 2.6 Kb using a linearized pUC-14S rRNA template. Reactions were pre-incubated with DNA, ymtRNAP, Mtf1, 2 mM $MgCl_2$, ATP, UTP and GTP for 5 minutes to allow RNAP binding and transcription initiation. CTP and 0.01 mg/mL of heparin (to inhibit reinitiation) were then added. Samples were loaded onto a denaturing formaldehyde gel, which was dried and exposed to a phosphor-screen (**B**) Percentage of the total transcript signal for each mutant with reference to wild-type (considered as 100%). Error bars indicate SE for 3 independent experiments.

The thumb subdomain is involved in Mtf1 binding

The interface between ymtRNAP and Mtf1 is not completely defined but deletions in the N-terminal domain of ymtRNAP weaken the interactions with Mtf1.[8] Since the thumb subdomain is adjacent to the N-terminal domain we were curious to see if thumb mutants affected this interaction. In our standard transcription reactions Mtf1 was maintained at 20-fold molar excess over ymtRNAP (**Fig. 2**). Since wild-type ymtRNAP and Mtf1 form a 1:1 complex and this interaction is necessary for transcription on duplex promoters, we decided to assay run-off transcription reactions with increasing concentrations of Mtf1, from 1 to 16-molar excess. The rationale for this experiment is that if thumb mutants are deficient in Mtf1 binding, then increasing Mtf1 concentrations should at least partially correct the deficits in thumb mutant activity. We observed that the total amount of run-off transcription is not altered as the Mtf1 concentration was increased from 1 to 16-fold excess in reactions with wild-type polymerase or the point mutants (**Fig. 7A, lane 1 to 5 and data not shown**). However, the thumb deletion mutants required a 4-fold molar excess of Mtf1 to reach the maximum level of transcript synthesis (**Fig. 7A, lanes 8 and 14**). As observed in **Figure 2**, wild-type ymtRNAP transcribed the expected 35-mer run-off product, whereas deletions in the thumb subdomain transcribed longer RNA products (**Fig. 7A**). To more directly identify possible binding defects between the deletion mutants and Mtf1, we performed an electrophoretic mobility shift assay (EMSA) assay with fixed concentrations of ymtRNAP and increasing concentrations of Mtf1 and a duplex 14S rRNA promoter. As previously reported, wild-type ymtRNAP shifts the labeled probe at 1:1 molar ratio of Mtf1.[9] However, TH_Δ5 requires a 4-fold excess of Mtf1 to shift the probe, and TH_Δ11 requires a 16-fold excess. The apparent K_d (measured as the interaction of the ymtRNAP-Mtf1 complex with a DNA template) for wild-type, TH_Δ5, and TH_Δ11 RNAPs on a duplex template were found to be 0.5×10^{-6} M, 1.5×10^{-6} M, and 5×10^{-6} M respectively (**Fig. 7B**). To see if these the observed binding differences are due to an interaction between Mtf1 and the RNAPs, and not due to the ability of the thumb mutant RNA polymerases to bind the promoter, we performed the same EMSA assay with a 'pre-melted' promoter (containing mismatches between the T- and NT-strands) (**Fig. 7C**). On such promoters, Mtf1 is not required for promoter melting. In contrast to the apparent dissociation constants on a duplex promoter in which the wild-type and TH_Δ11 K_d values differ by 10-fold, the apparent dissociation constants on a pre-melted promoter were 0.14×10^{-6} M, 0.16×10^{-6} M and 0.21×10^{-6} M for wild-type, TH_Δ5 and TH_Δ11 mutants respectively. We also measured the affinity of Mtf1 for the RNAPs by ultrafiltration of reactions with equimolar ymtRNAP and Mtf 1through membranes with 100 kDa MW cut-offs. Retenate and filtrates were collected and analyzed on 10% SDS PAGE (**Fig. 8**). In reactions with wild-type (**Fig. 9, lanes 2 and 3**) or the thumb point mutants (data not shown) all the Mtf1 is present in the retenate.[9] The deletion mutants, however, were deficient in interacting with Mtf1 as all detectable Mtf1 was found in the filtrate (**Fig. 8, lanes 6 and 9**).

Discussion

Rationale for targeting a region on helix N of the ymtRNAP subdomain for structure-function analysis

Structural and biochemical data from human mitochondrial and T7 RNA polymerases indicate that the thumb subdomain mediates elongation complex stability via the interaction with positively charged amino acids with the sugar-phosphate backbone of the RNA:DNA hybrid.[3,14,15,22] In contrast to those RNA polymerases, no structural information for ymtRNAP has been obtained to date. Thus, structure-function hyphothesis on ymtRNAP are driven by structural models and amino acid alignments.[8,9] Crystal structures of elongation complexes of T7RNAP show that residues R386 to R394 are involved in stabilizing a 7-base pair RNA:DNA hybrid,[22] whereas residues K767 to E788

stabilize a 9-base pair RNA:DNA hybrid in human mitochondrial RNA polymerase.[3] In human mitochondrial RNA polymerase, residues H748 to Q766 of the thumb subdomain contact DNA 10 to 13 base-pairs upstream of the RNA 3′-end, whereas in the T7RNAP elongation complex this region of the upstream DNA contacts the N-terminal domain. Thus, differences in the architecture of the transcription bubble and location of the upstream DNA mean that the thumb subdomain of hmtRNAP makes more DNA interactions than its T7RNAP counterpart. A structural alignment of ymtRNAP with T7RNAP and hmtRNAP indicates that the thumb subdomain of ymtRNAP is comprised of residues 737 to 813 (**Fig. 1**) and places a set of positively charged amino acids close to the center of αN of the thumb subdomain. Based on this structural alignment and taking into account the structural differences between T7RNAP and hmtRNAP elongation complexes, we constructed thumb subdomain mutants of ymtRNAP distributed across an interval of 20 amino acids (from R780 to R800) (**Fig. 1**).

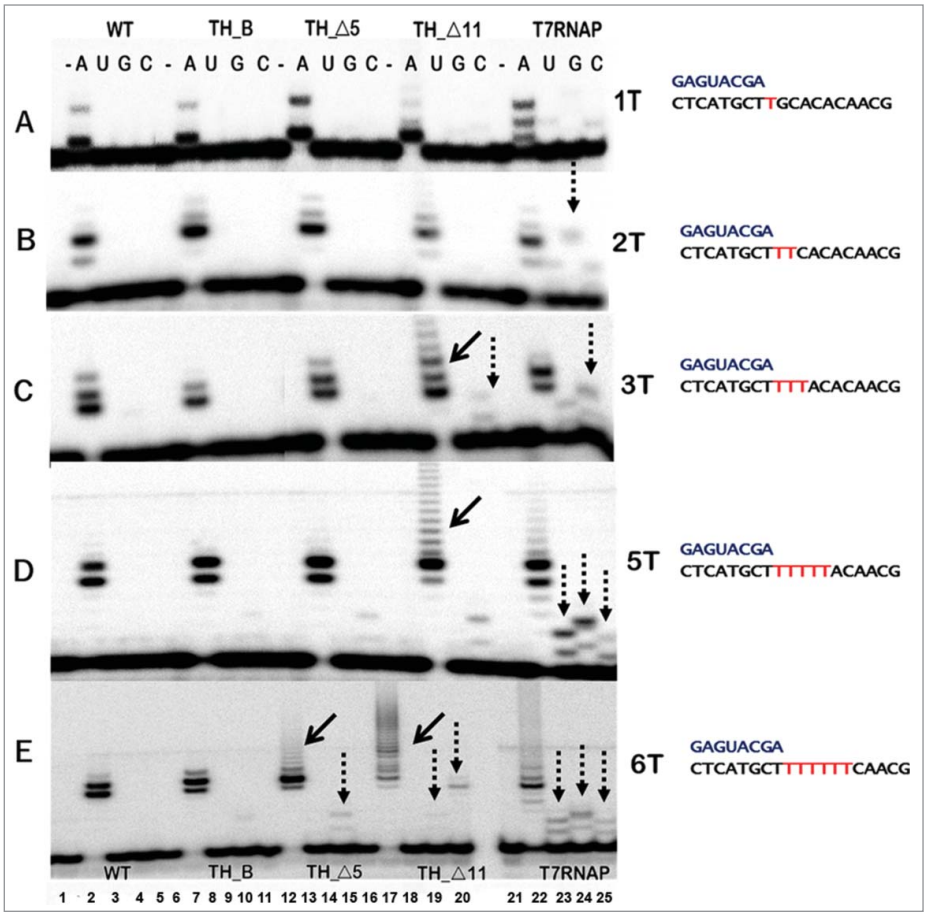

Figure 6. Frameshifting by transcriptional slippage is increased in thumb deletion mutants. Right Side: Representative experiment for determining frame-shift fidelity by wild-type and mutant RNAPs. Each panel (**A–D**) contains the following experimental setup: no NTPs (–), ATP (A), UTP (U), GTP (G) or CTP (C). RNA polymerases were assayed in the following order: WT, TH_B, TH_Δ5, TH_Δ11, and T7RNAP. Reactions were performed in the presence of 0.1 μM enzyme and 0.05 μM template. Panels from A (scaffold with one thymine) to E (scaffold with 6 thymines) correspond to templates with increasing runs of thymines. Solids arrows indicate frameshift errors, and dotted arrows indicate base substitution errors. Left Side: Graphical Representation of the RNA:DNA scaffolds. RNA probe in blue, DNA probe in black, thymine homopolymers in red.

The thumb subdomain is involved in complex stability

Thumb subdomain mutants and wild-type ymtRNAP displayed similar run-off transcriptional activity on a 35-mer template. However, point and deletion mutations increased the synthesis of abortive transcripts, indicating that they weaken initial transcription complex (**Fig. 2**). Deletions in the thumb subdomain also increased the addition of extra nucleotides at the 3' end of the run-off transcript. It is interesting to note that different single-subunit RNA polymerases have different propensities for extra 3′ NMP incorporation. For instance, in T7RNAP 15 to 70% of the transcripts can contain extra nucleotides, whereas RNAP from bacteriophage Syn5 does not incorporate extra nucleotides.[23,24] As bacteriophage Syn5 RNAP is more processive than T7RNAP, it is possible that the addition of extra nucleotides in thumb mutants is due to an RNA:template strand misalignment, suggesting that an enzyme defective in interactions with the RNA:DNA hybrid would increase extra nucleotide addition.[25]

Transcription reactions are divided into an early initiation (~2–5mer), late initial transcription (~6–12mer) and elongation (>~8–14mers; the specific base lengths at which these phases transition can vary for different RNAPs or promoters). The thumb subdomain of T7RNAP does not detectably stabilize the early ITC at the 2-mer stage as assessed by the effects of thumb mutations on turnover.[14,21] In the case of ymtRNAP, TH_A mutation did not affect 2-mer synthesis rates, while the TH_B and TH_C mutants increased 2-mer synthesis by ~2-fold (**Fig. 3A**), suggesting that while the ymtRNAP thumb may interact with RNAs as short as 2 nts, the contribution of the thumb subdomain to the stability of the 2-mer initial complex is minimal. This is in agreement with a crystal structure of a T7RNAP initial transcription complex with a 3-mer RNA, which reveals the thumb positioned to interact with RNA:DNA hybrids longer than 4-nt, but not with 2- or 3-mers,[26] and with biochemical experiments showing that the thumb subdomain of ymtRNAP is not involved in stabilizing an early ITC.[14] In contrast to the minimal effect of thumb mutations on 2-mer synthesis, thumb mutants increased the turnover of the late ITC 7-mer by 2–8

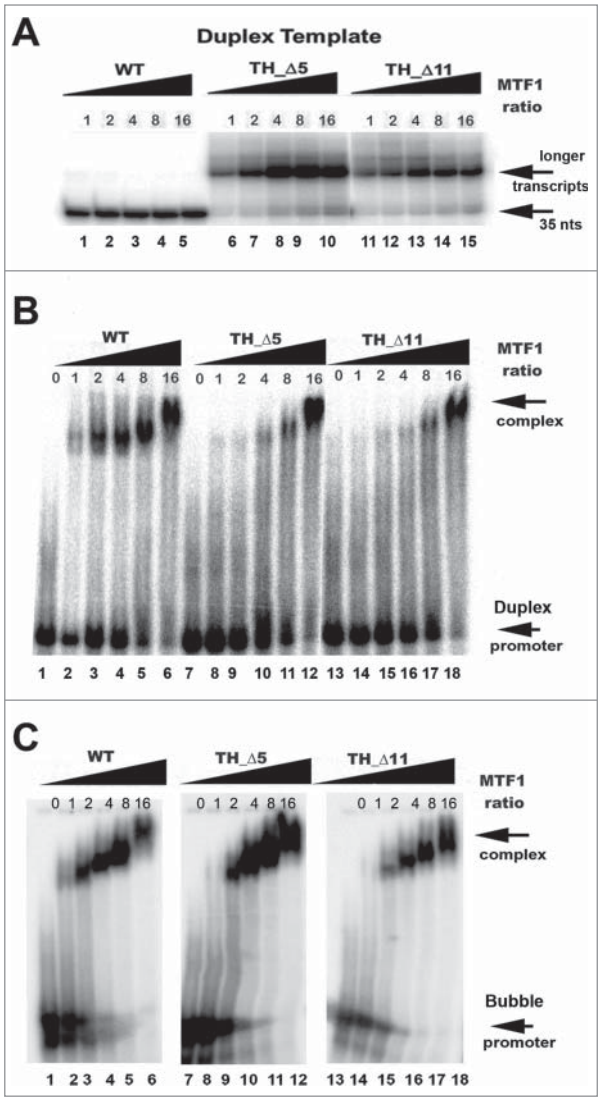

Figure 7. Thumb subdomain mutants shown reduced activity and complex formation with limiting amounts of Mtf1. (**A**) Representative run-off experiment for wild-type and thumb deletion mutants and increasing Mtf1 concentrations. The ratio of Mtf1 to ymtRNAP mutants was varied from 1 to 16 fold. The run-off product (35-mer) and longer RNA products are indicated by arrows. In the reactions in which wild-type ymtRNAP is present the synthesis of RNA does not change as the concentration of Mtf1 is increased. However, the thumb deletion mutants need 4-fold excess of Mtf1 to reach achieve the maximal amount of synthesis. Differences in transcript length (**Fig. 7A** lanes 1–5 vs lanes 8–14) correspond to aberrant transcripts synthesized by thumb mutants (as observed in **Fig. 2**). (**B**) Electrophoretic mobility shift assay with wild-type and deletion mutants on synthetic double stranded 14S rRNA promoters with increasing Mtf1:ymtRNAP ratios as in panel A. Wild-type ymtRNAP forms a complex with Mtf1 at 1:1 molar ratio, however deletion mutants require 4-fold (TH_Δ5) or 8-fold (TH_Δ11) excess of Mtf1. **C.** Electrophoretic mobility shift assay with wild-type and deletion mutants on a synthetic pre-melted 14S rRNA promoter with increasing RNAP concentrations.

fold, with TH_B and Δ11 mutants forming most unstable complexes (**Fig. 3D**). The T7RNAP-based model for the late ymtRNAP IC (**Fig. 3F**), indicates that the 2 residues mutated in

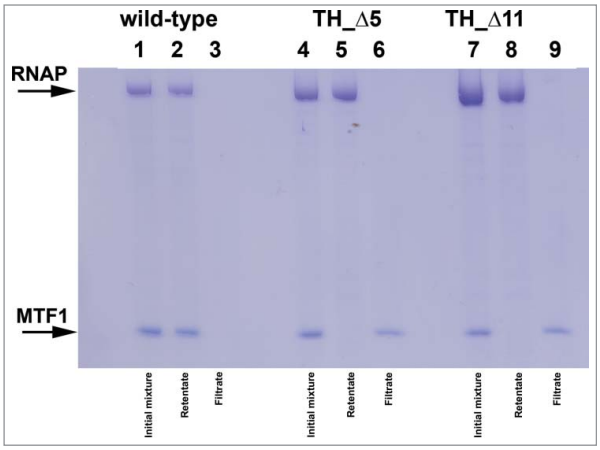

Figure 8. MTF1 binding to wild-type **and deletion mutants assessed by ultra-filtration**. Equimolar mixtures of wild type, TH_ Δ5 or TH_Δ11 ymtRNAPs with Mtf1 were mixed in transcription buffer and filtered through a 100 kDa MW cut-off Microcon centrifugal filter unit. Samples were analyzed by 10% SDS-PAGE. Unfiltered reactions corresponding to wild type, TH_ Δ5, TH_Δ11 yeast mtRNAPs with Mtf1 are in lanes 1, 4 and 7. Retentates were run in lanes 2, 5 and 8, and filtrates in lanes 3, 6, and 9.

TH_B (K787 and K792) are positioned to interact with the -4 and -5 nucleotides of the RNA:DNA hybrid. We also observed that the thumb mutants increase turnover of a halted 12-mer $_{EC}$ with respect to the wild-type enzyme. This effect is specially observed on super-coiled templates (**Fig.** 4). This may be because

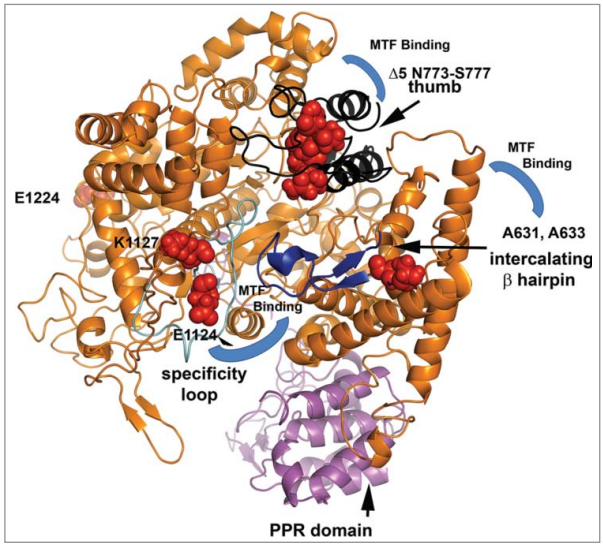

Figure 9. Homology model of ymtRNAP showing mutants that alter MTF1 binding. Ribbon representation of ymtRNAP based on the crystal structure of the elongation complex of hmtRNAP. The putative PPR domain is colored in purple, and the RNA polymerase domain is colored in orange. Point mutations that decrease the interaction between ymtRNAP and Mtf1 are located on the promoter specificity loop, intercalating β-hairpin and thumb subdomain. Amino acids whose mutation weakens the interaction between ymtRNAP and Mtf1 are in space filling representation.

transcription on supercoiled templates results in ECs with extended RNA:DNA hybrids which disrupt interactions between the normally single-stranded RNA and the RNAP. This disruption, coupled with mutations in the thumb, results in $_{EC}$ instability, as shown previously for T7RNAP.[21] In contrast, a large deletion of 40 amino acids in the hmtRNAP thumb exhibits a decrease in complex stability mainly at high salt concentrations.[3]

The thumb subdomain is important for frame-shift fidelity

Mutations in the thumb subdomains of DNAP decrease frame-shift fidelity.[17,27] Because of the appearance of longer aberrant transcripts in run-off transcription reactions in our thumb mutants, we tested their fidelity on templates with runs of thymines, which have been shown to cause frame-shifts during transcription or replication. We found that deletions in the thumb subdomain increase the number of AMPs incorporated at thymine runs. This phenomena starts with a run of 3 thymines, and AMP incorporation is seen to increase as the length of the thymine run increases (**Fig. 6**). In yeast and bacterial multi-subunit RNAP, mutants that increase transcript slippage map to residues involved in stabilizing the RNA:DNA hybrid of the $_{EC}$.[28,29]

The thumb subdomain is involved in Mtf1 binding

Mtf1 is a 341 amino acid protein homologous to rRNA methyltransferases, and consists of an α-β domain, a 4 helix domain and a disordered 17 amino acid C-terminal region.[30] The binding surface between ymtRNAP and Mtf1 is not fully defined and ymtRNAP mutants that are deficient in binding to Mtf1 are distributed across the polymerase in regions that are far from each other.[8,31,32] ymtRNAP is unable to melt a double stranded promoter in the absence of Mtf1. We determined if thumb mutants would have an effect on Mtf1 binding, and found that deletions of 5 and 11 amino acids in the thumb subdomain of ymtRNAP exhibit weakened Mtf1 binding as assed by EMSA and ultra-filtration experiments (**Figs. 7 and 8**). On a model of ymtRNAPs based on the elongation complex of hmtRNAP (**Fig. 9**), amino acids that decrease Mtf1 binding when mutated span multiple regions of ymtRNAP including the N-terminal region, and the promoter specificity and intercalating β-hairpin loops.[8,31,32] As the thumb subdomain is located near the intercalating hairpin and N-terminal domain, a contribution of the thumb subdomain to Mtf1 interaction is structurally reasonable, and consistent with recent EM studies of the human mitochondrial transcription initiation complex and the Mtf1 ortholog (TFB2M)[33] and of the ymtRNAP ITC.[34]

Material and Methods

Molecular biology methods

Mutant ymtRNAPs were constructed using Quick-Change directed mutagenesis kit as previously described.[10] Wild-type and mutant ymtRNAPs were over-expressed in *E. coli* BL21 (DE3) Star and purified as previously described.[9]

Transcription assays

Transcription (run-off) reactions (15 μL volume) were conducted at room temperature for 15 min in 20 mM Tris-HCl (pH 8.0), 4 mM $MgCl_2$, 10 mM DTT, and 50 mM NaCl (Transcription Buffer) with synthetic promoter templates at 0.05 μM, ymtRNAPs at 0.3 μM and Mtf1 (when present) at 1.8 μM, NTPs at 0.5 mM, and 0.1 μCi/μL of 3000 Ci/mM ^{32}P-α- ATP to label the transcripts. One to one volume of 98% formamide - 100 μM EDTA (stop buffer) was used to stop the reaction. Transcription reactions were resolved by denaturing polyacrylamide gel electrophoresis and quantified on a Molecular Dynamics Storm Phosporimager. Synthetic promoter templates with modified 14S mitochondrial promoter sequences were used in these reactions. The oligonucleotide sequences to assemble the 14S duplex promoter (annealing of 14S−NT + 14ST) were previously described.[9,10]

Stability on supercoiled versus linear template experiments was measured at room temperature following the conditions described above except that only ATP (2-mer complex) or ATP and UTP were added to the master mix, and the reaction was sampled at different incubation times as indicated in figure legends. Templates used for these experiments were constructed by annealing of oligonucleotides (14Sn_T and 14Sn_NT). These oligonucleotides have the 14S native promoter sequence reported previously[35] but with restriction sites for *Eco*RI and *BamH* I at their 5' and 3' ends, respectively. After annealing, the probe was digested and cloned into pUC19 between the *Eco*RI and *BamH* I restriction sites to create pUC19–14S. Linear versions of this template were generated by digestion with *Hind* III enzyme. Reagents and enzymes for cloning were from Thermo Scientific and, oligonucleotide sequences were as described in supplementary data.

Termination experiments were done using the same conditions as for the run-off experiments, but with a different set of promoters: pUC-14S was digested with *BamH* I and *Sca* I, and the hybridized products were subcloned into these restriction sites, producing 2 new template sequences: 14S-T7term-pUC (14S promoter and T7 termination signal) and pUC-14S- extended. These promoters were used as templates in an amplification reaction with Pfu polymerase (Thermo Scientific) using the primers pUC19_FW and *Hind* III_RW in order to generate the template for termination experiments. Reaction conditions were as follows: 50 ng/μL of amplified template, 0.3 μM ymtRNAP and 1.5 μM Mtf1 in a final volume of 20 μL.

Frameshift fidelity experiments were performed as described by Temiakov and coworkers[36] but with the following modifications: DNA promoters were constructed to hybridize with an 8 base RNA (supplementary data) and at the 3' end of the hybridization sequence one thymine residue was added to create the 1T template. This process was repeated to construct templates 2T, 3T, 5T and 6T containing increasing numbers of thymines. Transcription reactions contained template at a concentration of 0.1 μM, RNAPs at 0.5 μM, and 100 μM of each NTP. Reactions were stopped

with formamide-EDTA buffer. Transcription reactions on linearized and supercoiled plasmids were conducted based on the protocol described previously[37] except that the ymtRNAPs and Mtf1 concentration and transcription buffer were as described for the run off experiments. Transcription products were resolved on 1% agarose-formaldehyde gels. The gel was dried and exposed on a phosphor-screen for visualization and analysis.

Electrophoretic mobility shift assay

Electrophoretic mobility shift analysis experiments were conducted with duplex or pre-melted 14S rRNA promoters. Reaction mixtures contained fixed amounts of ymtRNAP and synthetic promoter DNA (0.2 and 0.02 μM respectively) incubated with increasing concentrations of Mtf1 (from 0.2 μM to 3.2 μM). Reactions were incubated in 20 mM Tris-HCl (pH 8.0), 75 mM NaCl, 5 mM DTT, 1 mM EDTA, and 10% glycerol for 10 minutes and resolved on an 8% native acrylamide gel. Data were fit to a quadratic equation to determine the equilibrium dissociation constant (K_d).

Structural Modeling

The structure of the elongation complex of ymtRNAP was based on the crystal structures of the initiation and elongation complexes of T7RNAP and the elongation complex of human mitochondria RNA polymerase. Ten initial models were built using the program MOE with the CHARMM22 force field.

Disclosure of Potential Conflicts of Interest

No potential conflicts of interest were disclosed.

Acknowledgements

We thank Xochitl Perez and Cei Abreu-Goodger for critical reading and Corina Diaz Quezada for technical support.

Funding

This work was supported by grants from the Howard Hughes Medical Institute and CONACYT (CB-2009–128647 and Problemas Nacionales 213915) to LGB.

References

1 Masters BS, Stohl LL, Clayton DA. Yeast mitochondrial RNA polymerase is homologous to those encoded by bacteriophages T3 and T7. Cell 1987; 51 89-99; PMID:3308116; http://dx.doi.org/10.1016/0092-8674(87)90013-4

2 Cermakian N, Ikeda TM, Cedergren R, Gray MW. Sequences homologous to yeast mitochondrial and bacteriophage T3 and T7 RNA polymerases are widespread throughout the eukaryotic lineage. Nucleic Acids Res 1996; 24:648-54; PMID:8604305; http://dx.doi.org/10.1093/nar/24.4.648

3 Schwinghammer K, Cheung AC, Morozov YI, Agaronyan K, Temiakov D, Cramer P. Structure of human mitochondrial RNA polymerase elongation complex. Nat Struct Mol Biol 2013; 20:1298-303; PMID:24096365; http://dx.doi.org/10.1038/nsmb.2683

4 Ringel R, Sologub M, Morozov YI, Litonin D, Cramer P, Temiakov D. Structure of human mitochondrial RNA polymerase. Nature 2011; 478:269-73; PMID:21947009; http://dx.doi.org/10.1038/nature10435

5 Steitz TA. The structural changes of T7 RNA polymerase from transcription initiation to elongation. Curr Opin Struct Biol 2009; 19:683-90; PMID:19811903; http://dx.doi.org/10.1016/j.sbi.2009.09.001

6 Durniak KJ, Bailey S, Steitz TA. The structure of a transcribing T7 RNA polymerase in transition from initiation to elongation. Science 2008; 322:553-7; PMID:18948533; http://dx.doi.org/10.1126/science.1163433

7 Rodeheffer MS, Shadel GS. Multiple interactions involving the amino-terminal domain of yeast mtRNA polymerase determine the efficiency of mitochondrial protein synthesis. J Biol Chem 2003; 278:18695-701; PMID:12637560; http://dx.doi.org/10.1074/jbc.M301399200

8 Paratkar S, Deshpande AP, Tang GQ, Patel SS. The N-terminal domain of the yeast mitochondrial RNA polymerase regulates multiple steps of transcription. J Biol Chem 2011; 286:16109-20; PMID:21454631; http://dx.doi.org/10.1074/jbc.M111.228023

9 Velazquez G, Guo Q, Wang L, Brieba LG, Sousa R. Conservation of promoter melting mechanisms in divergent regions of the single-subunit RNA polymerases. Biochemistry 2012; 51:3901-10; PMID:22524540; http://dx.doi.org/10.1021/bi300074j

10 Nayak D, Guo Q, Sousa R. A promoter recognition mechanism common to yeast mitochondrial and phage t7 RNA polymerases. J Biol Chem 2009; 284:13641-7; PMID:19307179; http://dx.doi.org/10.1074/jbc.M900718200

11 Brieba LG, Sousa R. The T7 RNA polymerase intercalating hairpin is important for promoter opening during initiation but not for RNA displacement or transcription bubble stability during elongation. Biochemistry 2001; 40:3882-90; PMID:11300767; http://dx.doi.org/10.1021/bi002716c

12 Karlok MA, Jang SH, Jaehning JA. Mutations in the yeast mitochondrial RNA polymerase specificity factor, Mtf1, verify an essential role in promoter utilization. J Biol Chem 2002; 277:28143-9; PMID:12021282; http://dx.doi.org/10.1074/jbc.M204123200

13 Paratkar S, Patel SS. Mitochondrial transcription factor Mtf1 traps the unwound non-template strand to facilitate open complex formation. J Biol Chem 2010; 285:3949-56; PMID:20008320; http://dx.doi.org/10.1074/jbc.M109.050732

14 Brieba LG, Gopal V, Sousa R. Scanning mutagenesis reveals roles for helix n of the bacteriophage T7 RNA polymerase thumb subdomain in transcription complex stability, pausing, and termination. J Biol Chem 2001; 276:10306-13; PMID:11124963; http://dx.doi.org/10.1074/jbc.M009866200

15 Bonner G, Lafer EM, Sousa R. The thumb subdomain of T7 RNA polymerase functions to stabilize the ternary complex during processive transcription. J Biol Chem 1994; 269:25129-36; PMID:7523379

16 Akabayov B, Akabayov SR, Lee SJ, Tabor S, Kulczyk AW, Richardson CC. Conformational dynamics of bacteriophage T7 DNA polymerase and its processivity factor, Escherichia coli thioredoxin. Proc Natl Acad Sci U S A 2010; 107:15033-8; PMID:20696935; http://dx.doi.org/10.1073/pnas.1010141107

17 Minnick DT, Astatke M, Joyce CM, Kunkel TA. A thumb subdomain mutant of the large fragment of Escherichia coli DNA polymerase I with reduced DNA binding affinity, processivity, and frameshift fidelity. J Biol Chem 1996; 271:24954-61; PMID:8798775; http://dx.doi.org/10.1074/jbc.271.40.24954

18 Chowdhury K, Tabor S, Richardson CC. A unique loop in the DNA-binding crevice of bacteriophage T7 DNA polymerase influences primer utilization. Proc Natl Acad Sci U S A 2000; 97:12469-74; PMID:11050188; http://dx.doi.org/10.1073/pnas.230448397

19 Mukherjee S, Brieba LG, Sousa R. Discontinuous movement and conformational change during pausing and termination by T7 RNA polymerase. Embo J 2003; 22:6483-93; PMID:14657021; http://dx.doi.org/10.1093/emboj/cdg618

20 Yin YW, Steitz TA. Structural basis for the transition from initiation to elongation transcription in T7 RNA polymerase. Science 2002; 298:1387-95; PMID:12242451; http://dx.doi.org/10.1126/science.1077464

21 Gopal V, Brieba LG, Guajardo R, McAllister WT, Sousa R. Characterization of structural features important for T7 RNAP elongation complex stability reveals competing complex conformations and a role for the non-template strand in RNA displacement. J Mol Biol 1999; 290:411-31; PMID:10390341; http://dx.doi.org/10.1006/jmbi.1999.2836

22 Yin YW, Steitz TA. The structural mechanism of translocation and helicase activity in T7 RNA polymerase. Cell 2004; 116:393-404; PMID:15016374; http://dx.doi.org/10.1016/S0092-8674(04)00120-5

23 Zhu B, Tabor S, Richardson CC. Syn5 RNA polymerase synthesizes precise run-off RNA products. Nucleic Acids Res 2013

24 Triana-Alonso FJ, Dabrowski M, Wadzack J, Nierhaus KH. Self-coded 3′-extension of run-off transcripts produces aberrant products during in vitro transcription with T7 RNA polymerase. J Biol Chem 1995; 270:6298-307; PMID:7534310; http://dx.doi.org/10.1074/jbc.270.11.6298

25 Zhu B, Tabor S, Raytcheva DA, Hernandez A, King JA, Richardson CC. The RNA polymerase of marine cyanophage Syn5. J Biol Chem 2013; 288:3545-52; PMID:23258537; http://dx.doi.org/10.1074/jbc.M112.442350

26 Cheetham GM, Jeruzalmi D, Steitz TA. Structural basis for initiation of transcription from an RNA polymerase-promoter complex. Nature 1999; 399:80-3; PMID:10331394; http://dx.doi.org/10.1038/19999

27 Bebenek K, Beard WA, Casas-Finet JR, Kim HR, Darden TA, Wilson SH, Kunkel TA. Reduced frameshift fidelity and processivity of HIV-1 reverse transcriptase mutants containing alanine substitutions in helix H of the thumb subdomain. J Biol Chem 1995; 270:19516-23; PMID:7543900; http://dx.doi.org/10.1074/jbc.270.33.19516

28 Zhou YN, Lubkowska L, Hui M, Court C, Chen S, Court DL, Strathern J, Jin DJ, Kashlev M. Isolation

and characterization of RNA polymerase rpoB mutations that alter transcription slippage during elongation in Escherichia coli. J Biol Chem 2013; 288:2700-10; PMID:23223236; http://dx.doi.org/10.1074/jbc.M112.429464

29 Strathern J, Malagon F, Irvin J, Gotte D, Shafer B, Kireeva M, Lubkowska L, Jin DJ, Kashlev M. The fidelity of transcription: RPB1 (RPO21) mutations that increase transcriptional slippage in S. cerevisiae. J Biol Chem 2013; 288:2689-99; PMID:23223234; http://dx.doi.org/10.1074/jbc.M112.429506

30 Schubot FD, Chen CJ, Rose JP, Dailey TA, Dailey HA, Wang BC. Crystal structure of the transcription factor sc-mtTFB offers insights into mitochondrial transcription. Protein Sci 2001; 10:1980-8; PMID:11567089; http://dx.doi.org/10.1110/ps.11201

31 Cliften PF, Jang SH, Jaehning JA. Identifying a core RNA polymerase surface critical for interactions with a sigma-like specificity factor. Mol Cell Biol 2000; 20:7013-23; PMID:10958696; http://dx.doi.org/10.1128/MCB.20.18.7013-7023.2000

32 Matsunaga M, Jaehning JA. A mutation in the yeast mitochondrial core RNA polymerase, Rpo41, confers defects in both specificity factor interaction and promoter utilization. J Biol Chem 2004; 279:2012-9; PMID:14570924; http://dx.doi.org/10.1074/jbc.M307819200

33 Yakubovskaya E, Guja KE, Eng ET, Choi WS, Mejia E, Beglov D, Lukin M, Kozakov D, Garcia-Diaz M. Organization of the human mitochondrial transcription initiation complex. Nucleic Acids Res 2014; 42:4100-12; PMID:24413562; http://dx.doi.org/10.1093/nar/gkt1360

34 Drakulic S, Wang L, Cuellar J, Guo Q, Velazquez G, Martin-Benito J, Sousa R, Valpuesta JM. Yeast mitochondrial RNAP conformational changes are regulated by interactions with the mitochondrial transcription factor. Nucleic Acids Res 2014; 42(17):11246-60; PMID:25183523; http://dx.doi.org/10.1093/nar/gku795

35 Marczynski GT, Schultz PW, Jaehning JA. Use of yeast nuclear DNA sequences to define the mitochondrial RNA polymerase promoter in vitro. Mol Cell Biol 1989; 9:3193-202; PMID:2677667

36 Temiakov D, Anikin M, McAllister WT. Characterization of T7 RNA polymerase transcription complexes assembled on nucleic acid scaffolds. J Biol Chem 2002; 277:47035-43; PMID:12351656; http://dx.doi.org/10.1074/jbc.M208923200

37 Wada T, Takagi T, Yamaguchi Y, Ferdous A, Imai T, Hirose S, Sugimoto S, Yano K, Hartzog GA, Winston F. DSIF, a novel transcription elongation factor that regulates RNA polymerase II processivity, is composed of human Spt4 and Spt5 homologs. Genes Dev 1998; 12:343-56; PMID:9450929; http://dx.doi.org/10.1101/gad.12.3.343